Frequency-Dependent Series Resistance of Monolithic Spiral Inductors

Min Park, *Member, IEEE*, Chung-Hwan Kim, Cheon Soo Kim, *Member, IEEE*, Mun-Yang Park, Sung-Do Kim, Young-Sik Youn, *Member, IEEE*, and Hyun Kyu Yu, *Member, IEEE*

***Abstract*—We present the analysis of the frequency dependent inductor series resistance (R_s). The high-frequency effects on series resistance have been confirmed with measured and simulated data of inductors having different geometric and process parameters in order to predict and optimize the high-performance inductors used in radio frequency (RF) integrated circuits (IC's). The results show that the magnetic field effect seems to be a dominant factor in determining the R_s in high-frequency region.**

***Index Terms*— Radio frequency (RF), series resistance, spiral inductor.**

I. Introduction

HIGH-FREQUENCY radio frequency (RF) integrated circuits (IC's) are crucial components of today's integrated system, since the full integration of transceivers for the wireless communication market is growing enormously in importance. The use of planar spiral inductors can improve these designs drastically: higher operating frequencies can be achieved, bandpass operation lowers the power consumption, and the use of low supply voltages is possible. The use of Si technology for the fabrication of inductors presents a difficult task, particularly in the integration of inductors without sacrificing the quality factor (Q) due to higher substrate losses [1]. Moreover, double-metal CMOS technology has been used with only two metal layers. This brings about a worst case technology for designing VCO's, since only two metal layers means the planar spiral inductor will have a large series resistance (R_s) compared to three- or four-level technologies. R_s is an important source of extra losses in high frequency. Therefore many approaches deviate from an analytical model of a planar spiral inductor on Si substrates [2], [3], but do not clearly to explain the behavior of R_s in the high-frequency region.

In this letter, the dependences of geometric and process parameters on R_s of spiral inductors have been analyzed in order to predict and optimize the performance of inductor in the high-frequency region.

II. Description of Inductors

A conventional CMOS technology with the double-metal of TiW/Al-1%Si/TiW interconnects was used to fabricate various spiral inductor structures [4]. In this work, geometric dimensions are 10–30-μm width and 2-μm spacing. The inner diameter (α) and number of turns (N) of inductor were variable with 20–180 μm and 4–12 turns, respectively. The metal coil layer for inductors was formed by the second metal layer, with total thickness of 1.1 and 3.1 μm [5]. We use a 625-μm-thick silicon wafer with the high-resistivity of 2 kΩcm. The substrate was grounded to make the inductors operate in CMOS RF IC's. S-parameters were measured on using on-wafer RF probes and a HP8510B Network Analyzer.

III. Results and Discussion

The measured Q of the inductor was determined as the ratio of the imaginary part to the real part of the one-port input impedance transformed from the measured two-port S-parameters. The measured two-port inductor parameters are determined uniquely from the Y-parameters converted from the measured and pad-deembedded S-parameters: $R_s = \text{Real}\ (-1/Y_{12})$ and $L = (1/\omega)\ \text{Imag}\ (-1/Y_{12})$ (equivalent circuit is indicated in Fig. 3(b) [6], [7]). In this circuit, L and R_s represent the series inductance and resistance, respectively. R_s also includes a frequency dependent term related to metal skin effect and other high-frequency effects. C_f models the parasitic capacitance which consists of the overlap capacitance between the spiral and the underpass, and fringing capacitance between adjacent metal lines. The effect of the fringing capacitance is small because the lines are almost equipotential. C_f is mainly attributed to the overlap capacitance due to the greater potential difference between them [8]. C_1 and C_2 represent the capacitance between the metal layer and the grounded substrate, and R_1 and R_2 model the resistance associated with the substrate losses. Model parameters were extracted by fitting the lumped model to the measured S-parameters using HP-EEsof LIBRA.

Fig. 1 shows the variation of R_s as a function of frequency. The R_s was calculated from the measured S-parameters. The α of inductor has been adjusted in order to achieve approximately the same inductance value. The ratio $R_s/R@dc$ is drawn, i.e., the ratio between the effective R_s at a certain frequency and the resistance at dc. At 2 GHz, the R_s of the first inductor (1) is already 50% higher than the value at dc, while the second one (2) only suffers a 30% increase. At even higher frequencies, the increase of resistance is enormous. Therefore, a smaller N of inductor is superior to higher N of inductor in order to obtain the high-performance inductor for high frequencies. This enormous difference cannot be explained

Manuscript received August 11, 1999; revised October 25, 1999. This work was supported by the Ministry of Information and Communications, Korea.

The authors are with the ETRI-Micro Electronics Technology Laboratory, Electronics and Telecommunications Research Institute, Taejon 305-350, Korea.

Publisher Item Identifier S 1051-8207(99)10320-9.

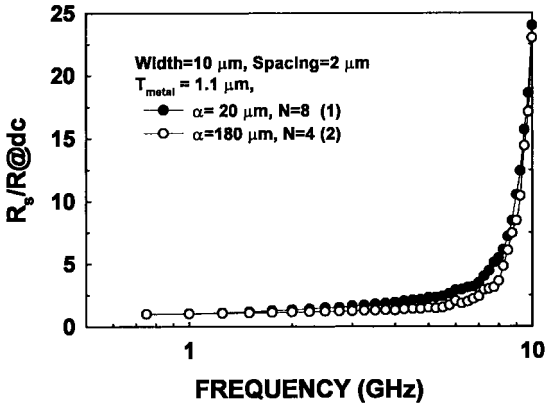

Fig. 1. Influence of the high-frequency effect on spiral inductor.

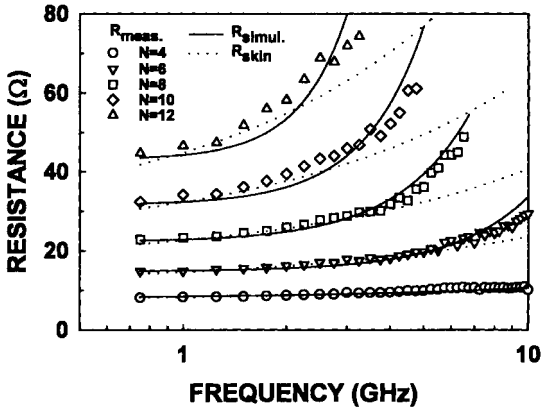

Fig. 2. Variation of the metal series resistance as a function of frequency.

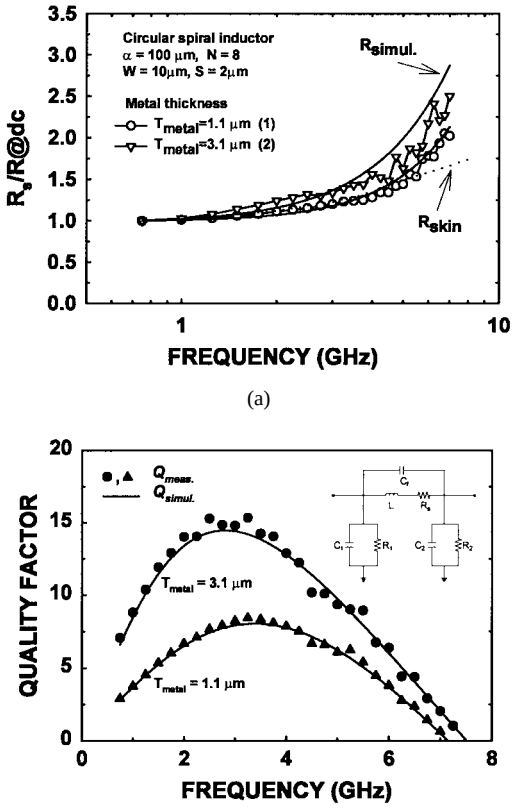

Fig. 3. (a) Frequency-dependent series resistance and (b) quality factor of circular spiral inductor with two kinds of metal thickness.

only by the skin effect in a single metal coil layer alone, since both layers are of equal width and they should suffer to the same amount from the nonuniform current distribution.

Fig. 2 shows the frequency-dependent R_s of inductors with various N. With increase of frequency, the measured series resistance $(R_{\text{meas.}})$ of the inductor with higher N is increased enormously. R_{skin} (dotted line) is the fitting value only using extended skin effect, related in (1), and $R_{simul.}$ (solid line) is the modified R_s with consideration of the both magnetic field and skin effect at high frequencies, related in (2).

At high frequencies, an estimate for R_s related to a planar inductor may be obtained from the following equation, which is extended with the frequency dependent skin effect [9]:

$$R_{skin} \approx \frac{l}{W \cdot \sigma \cdot \delta(1 - e^{-t/\delta})} \quad \text{and} \quad \delta = \sqrt{\frac{2}{\omega\mu\sigma}} \qquad (1)$$

where σ is the conductivity of the material, l is the total length of the winding, W and t are the width and thickness of the interconnect, and δ is the skin depth with μ the magnetic permeability of the material. In the planar inductor, this effect can no longer be calculated analytically, but it is clearly seen in the consideration of magnetic field effect in the addition of the skin effect.

When the spiral inductor is filled with turns up to the center of the coil, the induced eddy currents flow in a direction such that they oppose the original change in magnetic field that created them (negative feedback control loop in nature) [10]. These high-frequency effects are modeled using the following equation where A, B, C, and D are fitting parameters:

$$R_{simul.} \approx Af^{1/2}/[1 - e^{-Bf^{1/2}}] + Cf^{D}. \qquad (2)$$

As shown in Fig. 2, the frequency-dependent R_s shows good agreement with measured and fitted data.

Fig. 3(a) shows the influence of the high-frequency effect on a spiral inductor for two kinds of metal thickness. A small variation of $R_s/R@dc$ is shown in the low-frequency region. At 6 GHz, the R_s of the second inductor (2) is already 200% higher than the value at dc, while the first one (1) only suffers a 78% increase. The R_{skin} value of the 1st inductor is not matched with the value of $R_{simul.}$ above 5 GHz. The magnetic field effect seems to be a dominant factor in determining the R_s above this frequency. Such high-frequency effects as mentioned above are also shown in Fig. 3(b). The Q increases with the frequency up to the peak value and drops at higher frequencies due to the parasitic capacitance [11]. The differences of parasitic capacitances between two inductors are small as shown in Table I. However, the descending rate of Q after the maximum value of Q is different due to the deterioration of R_s. The solid lines indicate the simulated S-parameters by using HP-EEsof LIBRA optimization. As can be seen from the figure, simulated S-parameters match the measured ones well.

Fig. 4 shows the frequency dependence on R_s of inductors with different metal width. The ratio $R_s/R@dc$ increases with

TABLE I
SUMMARY OF EQUIVALENT CIRCUIT PARAMETERS FOR SPIRAL INDUCTORS

α (μm)	N	Q_{max}	f_{Qmax} (GHz)	f_{res} (GHz)	L (nH)	$R_{simul.}$ Model Para. A	B	C	D	R@dc (Ω)	A/B (Ω)	C_f (fF)	C_1 (fF)	C_2 (fF)	R_1 (KΩ)	R_2 (KΩ)	remark
100	12	4.74	1.5	3.25	34.05	1.48E-4	3.44E-6	1.205	3.115	43.87	43.02	30.73	33.62	66.32	15.56	7.46	(1)
100	10	6.57	2.25	4.75	21.98	2.53E-4	8.03E-6	0.798	2.510	32.09	31.51	28.55	19.36	48.49	20.0	7.65	(1)
100	8	6.47	2.75	6.50	13.09	5.08E-3	2.29E-4	0.600	2.088	22.69	22.18	24.02	19.28	34.44	18.89	8.18	(1)
100	6	7.43	4.25	10.50	6.80	2.95E-2	2.00E-3	0.190	1.995	14.52	14.75	19.19	13.84	23.25	15.39	8.90	(1)
100	4	10.59	11.25	19.75	2.79	8.67E-2	1.09E-2	0.457	0.730	8.47	7.95	12.85	9.02	13.62	10.74	9.01	(1)
20	8	7.3	5.5	12.25	5.39	2.99E-2	2.68E-3	1.108	1.296	11.20	11.16	16.95	12.15	21.90	21.0	8.90	(1)
180	4	9.25	6.0	13.25	5.25	8.08E-2	1.56E-2	3.998	0.586	5.20	5.18	15.92	11.59	17.06	18.1	9.71	(1)
100	8	8.44	3.25	7.0	11.96	2.06E-2	1.05E-3	0.357	2.130	20.22	19.62	21.64	19.55	28.36	19.85	7.28	(2)
100	8	15.34	3.25	7.25	11.85	2.34E-2	2.93E-3	0.419	1.862	7.84	7.99	19.11	18.74	28.38	22.52	7.09	(3)

*Remark: (1) Rectangular spiral inductor, T_{metal} = 1.1 μm (2) Circular spiral inductor, T_{metal} = 1.1 μm (3) Circular spiral inductor, T_{metal} = 3.1 μm

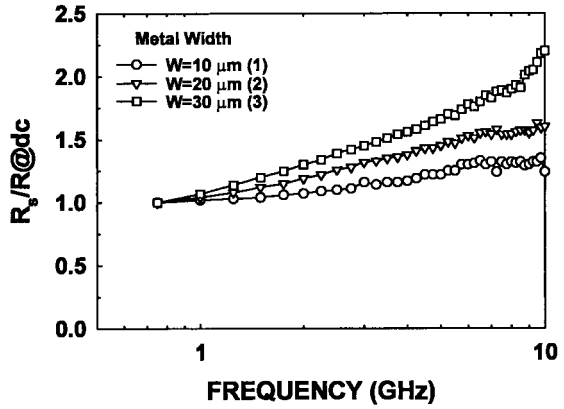

Fig. 4. Frequency dependence on series resistance of inductors with various metal widths.

increase of frequency. The ascending rate of $R_s/R@dc$ for wide metal width inductor is higher than that of $R_s/R@dc$ with narrow metal width. Moreover, the C_f value of the third inductor (3) is three times larger than the first one (1). Therefore, the performances of the inductor are degraded in high frequency. This proves that inductors using very wide metal turns are not the only way to go in designing high-Q inductors in the high-frequency region.

The summary of equivalent circuit parameters for the inductors is shown in Table I. With increasing N, the D value which is the main determining factor of induced magnetic field is increased. $R@dc$ represents the measured dc resistance. At low frequency (f approaches zero), frequency-dependent series resistance $R_{simul.}$ approaches about A/B and is similar with the value of $R@dc$. In higher N inductors, the magnetic field effect seems to be a dominant factor in increasing the R_s at high frequencies.

IV. CONCLUSIONS

We have studied the high-frequency effects on series resistance of inductors having different geometric and process parameters. In the case of an inductor with higher N, the magnetic field effect is a dominant fact in determining the series resistance in the high-frequency region. This is useful information in choosing inductor geometry, allowing designers to predict and optimize the performance of RF IC applications in the high-frequency region.

ACKNOWLEDGMENT

The authors would like to thank Mr. S. J. An for his technical contributions.

REFERENCES

[1] N. M. Nguyen and R. G. Meyer, "Si IC-compatible inductors and LC passive filters," *IEEE J. Solid-State Circuits*, vol. 25, pp. 1028–1031, Aug. 1990.
[2] C. P. Yue, C. Ryu, J. Lau, T. H. Lee, and S. S. Wong, "A physical model for planar spiral inductors on silicon," in *IEDM Tech. Dig.*, San Francisco, CA, Dec. 1996, pp. 155–158.
[3] J. R. Long and M. A. Copeland, "The modeling, characterization, and design of monolithic inductors for silicon RF IC's," *IEEE J. Solid-State Circuits*, vol. 32, pp. 357–369, Mar. 1997.
[4] M. Park, S. Lee, H. K. Yu, J. G. Koo, and K. S. Nam, "High Q CMOS-compatible microwave inductors using double-metal interconnection silicon technology," *IEEE Microwave Guided Wave Lett.*, vol. 7, pp. 45–47, Feb. 1997.
[5] M. Park, C. S. Kim, J. M. Park, H. K. Yu, and K. S. Nam, "High Q microwave inductors in CMOS double-metal technology and its substrate bias effects for 2 GHz RF IC's application," in *IEDM Tech. Dig.*, Washington, DC, Dec. 1997, pp. 59–62.
[6] P. J. van Wijnen, H. R. Claessen, and E. A. Wolsheimer, "A new straightforward calibration and correction procedure for "on wafer" high-frequency S-parameter measurements (45 MHz-18 GHz)," *IEEE Bipolar Circuits and Technol. Meet.*, 1987, pp. 70–73.
[7] S. Chaki, S. Aono, N. Andoh, Y. Sasaki, N. Tanino, and O. Ishihara, "Experimental study on spiral inductors," in *IEEE MTT-S Int. Microwave Symp. Dig.*, June 1995, pp. 753–756.
[8] L. Wiemer and R. H. Jansen, "Determination of coupling capacitance of underpass, air bridges and crossing in MIC's and MMIC's," *Electron. Lett.*, vol. 23, no. 7, pp. 344–346, Mar. 1987.
[9] T. H. Lee, *The Design of CMOS Radio-Frequency Integrated Circuits*. New York: Cambridge Univ. Press, 1988, ch. 2, pp. 50–51.
[10] J. Cranink and M. S. J. Steyaert, "A 1.8-GHz low-phase-noise CMOS VCO using optimized hollow spiral inductors," *IEEE J. Solid State Circuits*, vol. 32, pp. 736–744, May 1997.
[11] M. Park, S. Lee, C. S. Kim, H. K. Yu, and K. S. Nam, "The detailed analysis of high Q CMOS-compatible microwave spiral inductors in silicon technology," *IEEE Trans. Electron Devices*, vol. 45, pp. 1953–1959, Sept. 1998.